MOLECULAR CARCINOGENESIS 47:184–196 (2008)

Antitumor Activity of 3,5,4′-Trimethoxystilbene in COLO 205 Cells and Xenografts in SCID Mice

Min-Hsiung Pan,[1]* Jia-Hui Gao,[1] Ching-Shu Lai,[1,2] Ying-Jan Wang,[2] Wen-Ming Chen,[1] Chih-Yu Lo,[3] Mingfu Wang,[4] Slavik Dushenkov,[5] and Chi-Tang Ho[3]

[1]*Department of Seafood Science, National Kaohsiung Marine University, Kaohsiung, Taiwan*
[2]*Department of Environmental and Occupational Health, National Cheng Kung University Medical College, Tainan, Taiwan*
[3]*Department of Food Science, Rutgers University, New Brunswick, New Jersey*
[4]*Department of Botany, The University of Hong Kong, Pokfulam Road, Hong Kong, People's Republic of China*
[5]*WellGen, Inc., New Brunswick, New Jersey*

Resveratrol (R-3), a trihydroxy *trans*-stilbene from grape, inhibits multistage carcinogenesis in animal models. Here we report that 3,5,4′-trimethoxystilbene (MR-3), the permethylated derivative of R-3 was more potent against the growth of human cancer cells (HT-29, PC-3, COLO 205) with estimated IC_{50} values of 81.31,42.71, and 6.25 μM, respectively. We further observed that MR-3 induced apoptosis in COLO 205 cells through modulation of mitochondrial functions regulated by reactive oxygen species (ROS). ROS generation occurs in the early stages of MR-3-induced apoptosis, preceding cytochrome-*c* release, caspase activation, and DNA fragmentation. Significant therapeutic effects were demonstrated in vivo by treating severe combined immune deficiency (SCID) mice bearing COLO 205 tumor xenografts with MR-3 (50 mg/kg ip). Assays on DNA fragmentation and caspase activation were performed and demonstrated that apoptosis occurred in tumor tissues treated with MR-3. The appearance of apoptotic cells, as shown by Hematoxylin and Eosin (H&E) staining, and an increase in p21 and decrease in proliferating cell nuclear antigen (PCNA) protein by immuno-histochemistry were observed in tumor tissues under MR-3 treatment. Our study identifies the novel mechanisms of the antitumor effects of MR-3 and indicates that these results may have significant applications for cancer chemotherapy.

Key words: MR-3; apoptosis; cytochrome-c; caspase-9; caspase-3; p53; SCID mice

INTRODUCTION

Epidemiological studies have provided convincing evidence that dietary factors can modify the processes of carcinogenesis, including initiation, promotion, and progression of several types of human cancer [1]. The occurrence of gastrointestinal (GI) cancers has increased strikingly during the past decade. As an example, colorectal cancer is the second leading cause of cancer mortality in Western societies [2] and one of the world's most common malignancies [3,4]. The fight against GI cancer is an important global health issue.

Resveratrol (3,5,4′-trihydroxystilbene, Figure 1, R-3), a phytoalexin present in a variety of medicinal plants, grapes, peanuts, and pines, has been found to possess cancer chemopreventive activity through the inhibition of ribonucleotide reductase and cellular events associated with cell proliferation, tumor initiation, promotion, and progression [5–7]. Resveratrol has been shown to have growth-inhibitory activity in several human cancer cell lines and in animal models of carcinogenesis [8]. Moreover, resveratrol has been found to be a potential cancer chemotherapeutic agent, which can decrease tumor growth in a rat tumor model [9]. Previously, a study indicated that R-3 (3,5,4′-trihydroxystilbene, Figure 1) or its methoxy derivative, MR-3 (3,5,4′-trimethoxystilbene), inhibited the growth of both normal lung fibroblast WI38 cells, and the SV40 virally transformed WI 38 cells with equal efficacy [6]. However, the in vivo antitumor effect of MR-3 remains unclear.

Angiogenesis is clearly a central requirement for the unrestricted growth of a number of solid tumors [10]. Thus, chemical agents able to affect neo-vascularization may have broad applicability for

Abbreviations: R-3, resveratrol; MR-3, 3,5,4′-trimethoxystilbene; DFF, DNA fragmentation factor; PARP, poly(ADP-ribose) polymerase; Apaf-1, apoptotic protease activating factor 1; ICAD, inhibitor of caspase-3-activated DNase; DCHF-DA, dichlorodihydrofluorescein diacetate; DHE, dihydroethidium; CMFDA, 5-chloromethylfluorescein diacetate; PDTC, pyrrolidine dithiocarbamate; DPI, diphenylene iodonium; SOD, superoxide dismutase; ALL, allopurinol; ROS, reactive oxygen species; NAC, *N*-acetylcysteine; CAT, catalase; PCNA, proliferating cell nuclear antigen; H&E, hematoxylin and eosin; SCID, severe combined immune deficiency.

*Correspondence to: Department of Seafood Science, National Kaohsiung Marine University, No. 142, Hai-Chuan Rd, Nan-Tzu, Kaohsiung, Taiwan.

Received 6 January 2007; Revised 15 March 2007; Accepted 9 April 2007

DOI 10.1002/mc.20352

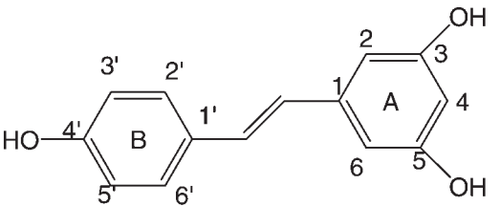

Resveratrol (R-3)
(3,5,4'-trihydroxy-*trans*-stilbene)

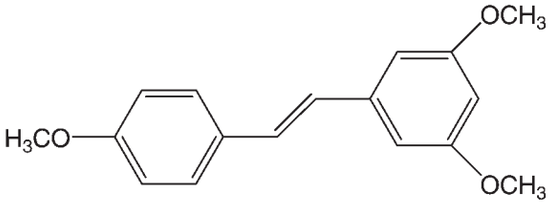

MR-3
(3,5,4'-trimethoxystilbene)

Figure 1. The chemical structures of resveratrol and MR-3.

the therapy of a wide spectrum of diseases involving pathologic angiogenesis, including cancer. MR-3 has anti-angiogenic and vascular-targeting activity, causing microtubule disassembly and tubulin depolymerization [11]. The present study focused on the identification of the structural determinants responsible for the antiproliferative activity of resveratrol and its methoxy derivative (R-3 and MR-3), both in vitro and in vivo.

Our results demonstrated that MR-3 exerts better antitumor activity than R-3 via apoptosis induction on human colorectal carcinoma COLO 205 cells. Apoptosis is an essential biochemical process required to defend the body against cancers, and in cancer, it is the process in which cells die in order to maintain homeostasis of inflammatory and immune responses to cancer cells [12–14]. Many recent studies have indicated that anticancer drugs or cancer chemopreventive agents act through the induction of apoptosis to prevent tumor promotion and progression. The process of apoptosis is orchestrated by the activation of ''executioner'' caspases, stored in most cells, as zymogens. Proteolytic cleavage activates the initiating zymogen, which in turn triggers sequential proteolytic activation of each successive pro-caspase in the apoptosis cascade [15,16]. Furthermore, it appears that a range of molecular affinities exist, which control the interactions between apoptosis family members, such as Bcl-2 (or Bcl-X_L) and Bax, to promote cell survival, or Bax-homodimer formation, which promotes cell death [17,18]. Current evidence suggests that Bcl-2 acts upstream of caspase-3 activation, at the level of cytochrome-*c* release, to prevent apoptosis [19]. It has been shown that the Bcl-2 and Bcl-X_L of mammals can be converted into potent pro-apoptotic molecules when they are cleaved by the caspases, resulting in accelerated cell apoptosis [19,20].

The current options for treating human cancer are limited to excision surgery, systemic chemotherapy, gene therapy, immunotherapy, radiation therapy, complementary therapy, and hormone therapy [21]. The ability of cancer chemotherapeutic agents to initiate apoptosis is an important determinant of their therapeutic response [22]. In this current study, we first examined the antiproliferative effects of resveratrol and its methoxy derivative on human cancer cells. Our results clearly demonstrated that MR-3 can induce apoptosis in a dose-dependent manner in COLO 205 cells.

We further evaluated the molecular mechanisms of apoptotic effects induced by MR-3. To elucidate the anticancer mechanism of MR-3, we investigated the production of ROS, the progression of changes in the Bcl-2 protein family, and caspase responses related to MR-3-induced apoptosis in human COLO 205 cancer cells. In vivo therapeutic efficacy was further examined by treating SCID mice bearing COLO 205 tumor xenografts with 50 mg/kg *ip* MR-3. This study provides novel evidence that the methoxy derivative (MR-3) of resveratrol is a potential chemotherapeutic agent.

MATERIALS AND METHODS

Cell Culture and Chemicals

The cell line COLO 205 (CCL-222; American Type Culture Collection) is developed from a poorly differentiated human colon adenocarcinoma [23]. The HT-29 cell line was isolated from human colon adenocarcinoma (ATCC HTB-38). The human prostate cancer PC-3 cell line was obtained from American Type culture Collection (ATCC, Manassas, VA). COLO 205 and HT-29 cells were grown in RPMI-1640 supplemented with 10% heat-inactivated fetal bovine serum (GIBCO BRL, Grand Island, NY), 100 units/mL of penicillin, 100 μg/mL of streptomycin), 2 mM L-glutamine (GIBCO BRL), and was maintained at 37°C in a humidified, 5% CO_2 incubator. PC-3 cells were cultured in F-12K medium, supplemented with 10% FBS and 2 mM L-glutamine. The inhibitor of caspase-3 (Z-Val-Ala-Asp-fluoromethyl ketone, Z-VAD-FMK) was purchased from Calbiochem (La Jolla, CA). Propidium iodide was obtained from Sigma Chemical Co. (St. Louis, MO). The synthesis of resveratrol using 4-methoxybenzyl alcohol and 3,5-dimethoxybenzaldehyde as precursors has been described [6]. A similar strategy was employed to prepare 3,5,4′-trimethoxystilbene.

Trypan Blue Exclusion Assay

Human cancer cells (5×10^4) were plated into 35-mm Petri dishes in RPMI-1640 medium. The next day, the medium was changed and various concentrations of R-3, and MR-3 were added. Control cells were treated with DMSO to yield a final concentration of 0.05% (v/v). At the end of incubation, cells were harvested by the trypsin procedure. Cells were then concentrated by centrifugation and were stained by trypan blue (Invitrogen, Renfrewshire, UK) for 10 min. Viable cells were counted in a hemocytometer [24].

DNA Extraction and Electrophoretic Analysis

The COLO 205 human cancer cells were harvested, washed with phosphate-buffered saline (PBS), and then lysed overnight at 56°C with a digestion buffer containing 0.5% sarkosyl, 0.5 mg/mL proteinase K, 50 mM tris(hydroxymethyl) aminomethan (pH 8.0), and 10 mM EDTA. Following lysis, the cells were then treated with RNase A (0.5 μg/mL) for 3 h at 56°C. The DNA was then extracted using phenol/chloroform/isoamyl alcohol (25:24:1) prior to loading, and was analyzed by 2% agarose gel electrophoresis. The agarose gels were run at 50 V for 120 minutes in Tris-borate/EDTA electrophoresis buffer (TBE). Approximately 20 μg of DNA was loaded in each well with 6× loading buffer containing 0.25% bromophenol blue, 0.25% xylene xyanol, and 40% sucrose. DNA was stained with ethidium bromide and visualized under UV light (wavelength, 260 nm), and the plates photographed [25].

Flow Cytometry

COLO 205 cells (2×10^5) were cultured in 60-mm Petri dishes in RPMI-1640 medium and incubated for 24 h. The cells were then harvested, washed with PBS, re-suspended in 200 μL of PBS, and fixed in 800 μL of 100% ethanol at −20°C. After being left to stand overnight, the cell pellets were collected by centrifugation, re-suspended in 1 mL of hypotonic buffer (0.5% Triton X-100 in PBS and 0.5 μg/mL RNase), and incubated at 37°C for 30 min. Next, 1 mL of propidium iodide solution (50 μg/mL) was added, and the mixture was allowed to stand on lump of ice for 30 min. Fluorescence emitted from the propidium iodide–DNA complex was quantitated after excitation of the fluorescent dye by FACScan cytometry (Becton Dickinson, San Jose, CA). Quantitation of the fraction of each cell cycle stage was performed with ModFit LT for Mac 3.0 software (Becton Dickinson).

ROS Production Determination

ROS production was monitored by flow cytometry using 2′,7′-dichlorodihydrofluorescein diacetate (DCFH-DA) and dihydroethidium (DHE). This dye is a stable, non-polar compound that readily diffuses into cells and is hydrolyzed by intracellular esterase to yield 2′,7′-dichlorodihydrofluorescein (DCFH), which is trapped within the cells. Hydrogen peroxide or low molecular weight peroxides produced by the cells oxidize DCFH to the highly fluorescent compound 2′,7′-dichlorofluorescein (DCF). DHE was used as a probe, recognizing mainly the oxygen species, superoxide anion. Thus, the fluorescence intensity is proportional to the amount of peroxide produced by the cells. Cells were treated with MR-3 (50 μM) for different time periods, and DCFH-DA (30 μM) was added into the medium for a further 30 min at 37°C.

Analysis of the Mitochondrial Trans-Membrane Potential

The change of the mitochondrial trans-membrane potential was monitored by flow cytometry. Briefly, COLO 205 cells were exposed to MR-3 (50 μM) for different time periods and the mitochondrial trans-membrane potential was measured directly using 40 nM 3,3′-dihexyloxacarbocyanine [DiOC6(3)] (Molecular Probes, Eugene, OR). Fluorescence was measured after staining the cells for 30 min at 37°C. Histograms were analyzed using Cell Quest software and were compared with histograms of untreated, control cells.

Western Blotting

For the determination of the expression of Bcl-2 family, p53, Fas, and FasL in COLO 205 cells, the nuclear and cytosolic proteins were isolated from COLO 205 cells in Petri dishes with a cell scraper following treatment with 50 μM MR-3 for 0, 3, 6, 9, 12, and 24 h. The total proteins were extracted via the addition of 200 μL of gold lysis buffer (50 mM Tris-HCl, pH 7.4, 1 mM NaF,150 mM NaCl,1 mM EGTA, 1 mM phenylmethanesulfonyl fluoride, 1% NP-40, and 10 μg/mL leupeptin) to the cell pellets on ice for 30 min, followed by centrifugation at 10,000g for 30 min at 4°C. The cytosolic fraction (supernatant) proteins were measured using a Bio-Rad protein assay kit (Catalog 500–0006, Bio-Rad Laboratories, Munich, Germany). The samples (50 μg of protein) were mixed with 5× sample buffer containing 0.3 M Tris-HCl (pH 6.8), 25% 2-mercaptoethanol, 12% sodium dodecyl sulfate (SDS), 25 mM EDTA, 20% glycerol, and 0.1% bromophenol blue. The mixtures were boiled at 100°C for 5 min and were pre-run on a stacking gel and then resolved by 12% SDS–polyacrylamide minigels at a constant current of 20 mA. Subsequent electrophoreses were routinely carried out on 12% SDS–polyacrylamide gels. Following electrophoresis, proteins on the gel were electro-transferred onto a 45 micron immobile membrane (PVDF; Millipore Corp., Bedford, MA) using a transfer buffer composed of 25 mM Tris-HCl (pH 8.9), 192 mM glycine, and 20% methanol. The membranes were blocked using a blocking solution (20 mM Tris-HCl pH 7.4, 0.2% Tween 20, 1% bovine

serum albumin, and 0.1% sodium azide). The membrane was then further incubated with respective, specific antibodies at appropriate dilutions (1: 1,000) using blocking solutions, such as anti-Bcl-2, anti-Bcl-X_L, anti-Bad, anti-Bax, anti-β-actin (Santa Cruz Biotech.), anti-PARP (UBI, Inc., Lake Placid, NY), anti-Bid, anti-p53 (Transduction Laboratory, Lexington, KY), and anti-DFF45/inhibitor of caspase-activated DNase (ICAD) antibody (MBL, Naka-Ku, Nagoya, Japan) at room temperature for 1 h. The membranes were subsequently probed with anti-mouse or anti-rabbit IgG antibody, conjugated with horseradish peroxidase (Transduction Laboratories, Lexington, KY) and detection was achieved by measuring the chemiluminescence of the blotting agent (ECL, Amersham Corp., Arlington Heights, IL) after exposure of the filters onto Kodak X-Omat films. The densities of the bands were quantitated with a computerized densitometer (AlphaImager™ 2200 System). The mitochondrial and cytosolic fractions isolated from the cells were used for immunoblot analysis of cytochrome-*c* as previously described [26]. The cytochrome-*c* protein was detected using an anti-cytochrome-*c* antibody (Research Diagnostic, Inc., Flanders, NJ).

Activity of Caspase

After MR-3 treatment, cells were collected and washed with PBS and suspended in 25 mM HEPES (pH 7.5), 5 mM $MgCl_2$, 5 mM EDTA, 5 mM dithiothione, 2 mM phenylmethanesulfonyl fluoride, 10 μg/mL pepstatin A, and 10 μg/mL leupeptin after treatment. Cell lysates were clarified by centrifugation at 12,000*g* for 20 min at 4°C. Caspase activity in the supernatant was determined by a fluorogenic assay (Promeaga's CaspACE Assay System Corp., Madison, WI). For quantitation of the protein concentrations, we used bovine serum albumin to develop the standard curve. Briefly, 50 μg of total protein, as determined by the Bio-Rad protein assay kit (Catalog 500-0006, Bio-Rad Laboratories), was incubated with 50 μM substrate Ac-Try-Val-Ala-Asp-AMC (Ac-YVAD-AMC, caspase-1-specific substrate), Ac-Asp-Glu-Val-Asp-AMC (Ac-DEVD-AMC, caspase-3-specific substrate), Ac-Ile-Glu-Thr-Asp-AMC (Ac-IETD-AMC, caspase-8-specific substrate), or Ac-Leu-Glu-His-Asp-AMC (Ac-LEHD-AMC, caspase-9-specific substrate) at 30°C for 1 h. The release of methylcoumaryl-7-amine (AMC) was measured by excitation at 360 and emission at 460 nm using a fluorescence spectrophotometer (Varian, Palo Alto, CA).

Treatment of COLO 205-Derived Xenografts, In Vivo

Male SCID mice (5-wk-old) (purchased from Tzu Chi University Animal Center, Hualien, ROC) were maintained in pathogen-free sterile isolators according to institutional guidelines, and all food, water, caging, and bedding were sterilized prior to use. All procedures were approved by the National Animal Care and Use Committee. The dorsal region of each SCID mouse was shaved with an electric clipper 2 days before transplantation. COLO 205 cells (5×10^6) in 0.2 mL PBS were injected subcutaneously between the scapulae of each SCID mouse. After transplantation, tumor size was measured using calipers and the tumor volume was estimated according to the following formula: tumor volume (mm^3) $= L \times W^2/2$, where L is the length and W is the width. Once tumors reached a mean size of 200 mm^3, animals received either 20 μL intra-peritoneal injections of corn oil (control group), or MR3 (50 mg/kg) three times per week (active group) for 23 days [27].

Immunohistochemical Staining

Paraffin-embedded blocks were sectioned at about 4-μm thickness, de-paraffinized, and re-hydrated. After microwave pretreatment in citrate buffer, pH 6.0, for antigen retrieval, slides were immersed in 0.3% hydrogen peroxide for 20 min to block the endogenous peroxidase activity. After intensive washing with PBS, slides were incubated overnight at 4°C with p53 or PCNA-specific antibodies (Santa Cruz Biotechnology) at a dilution of 1:50. After a second incubation with an alkaline phosphatase-conjugated, affinity-purified secondary-antibody (Chemicon Interational, Temecula, CA), followed by washing with PBS, reaction products were visualized by immersing slides in coloregenic substrates: nitro blue tetrazolium (NBT) and 5-bromo-4-cholro-3-indolylphosphate (BCIP), as suggested by the manufacturer (Sigma Chemical Co.), and finally counterstained with hematoxylin.

Statistical Analysis

Data are presented as means ± standard deviation (SD). Statistical significance was examined using the Student's *t*-test comparison between the means. A *P*-value of <0.05 was considered statistically significant.

RESULTS

Inhibition of Cell Proliferation in MR-3-Treated Human Cancer Cells

We first compared the effects of R-3 and MR-3 (Figure 1) on the growth of human cancer cells using the trypan blue exclusion assay as previously described. As shown in Figure 2, MR-3 decreased cell growth in cultured human cancer cells (HT-29, PC-3, and COLO 205) in a dose-dependent manner, with IC_{50} values of 81.31, 42.71, and 6.25 μM, respectively. The cell-growth inhibitory effect on COLO 205 cells (p53 wild-type) was sensitive to MR3 as compared to HT-29 (p53 mutant) and PC3 (p53 null). These results suggest that p53 could be a key

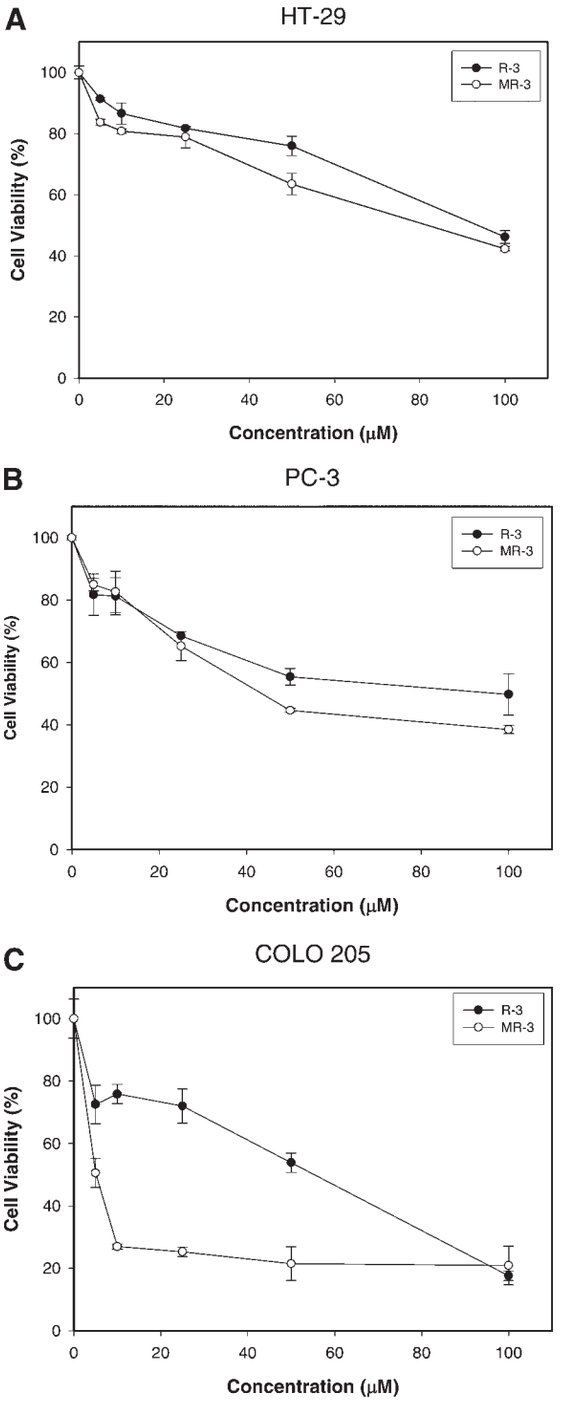

Figure 2. Effect of R-3 and MR-3 on the growth of various human cancer cells. Cells were treated with 0, 5, 10, 25, 50, 100 μM of the indicated compounds for 24 h. Cell viability then was determined by trypan blue exclusion assay as described. Data expressed as mean ± SD.

regulator in COLO 205 cells. Compared to R-3, MR-3 was a stronger inhibitor of COLO 205 cell growth. As a result, we further examined the cytotoxic effects of MR-3 in COLO 205 cells.

MR-3 Induces Apoptosis in Human Colorectal Carcinoma Cells

Physiological cell death is characterized by apoptotic morphology, including chromatin condensation, membrane blebbing, inter-nucleosomal degradation of DNA, and apoptotic body formation. To investigate whether the cytotoxic effects of MR-3 observed in COLO 205 cells were because of apoptotic cell death, cells were treated with MR-3 (5–100 μM) for 24 h and DNA fragmentation analyses were performed. As shown in Figure 3, significant DNA ladders were observed in COLO 205 cells after 50 μM of MR-3 treatment for 24 h. After treatment with 50 μM MR-3 for 12 h, digested genomic DNA was evident. DNA laddering was not observed in R-3-treated cells.

MR-3 Induction of Cleavage and Activation of Caspase Activity

The caspases are believed to play a major role in causing apoptosis by cleaving or degrading several cellular substrates [28]. To monitor the enzymatic activity of caspase-1, 3, 8, and 9, caspase activity was measured following treatment of COLO 205 cells with 50 μM MR-3 for several periods. As shown in Figure 4A, MR-3 induced a dramatic increase in caspase-9 activity of approximately 3.2-fold after 6 h of treatment. Furthermore, both caspase-3 and caspase-8 were activated in a time-dependent manner by MR-3, but the data showed only a very low level of caspase-1 activity following MR-3 treatment. Figure 4B shows the cleavage of pro-caspase-9 and pro-caspase-3 occurring at 3 h and sequentially in COLO 205 cells exposed in a time-dependent manner, whereas the cleavage of pro-caspase-8 occurred at 6 h in MR-3-treated COLO 205 cells. A time-dependent, proteolytic cleavage of caspases, with an increase of the cleavage fragment was associated with the activity of caspase.

Activation of caspase-3 causes the cleavage of poly-(ADP-ribose)-polymerase (PARP), a hallmark of apoptosis, and produces an 85 kDa fragment during apoptosis [29]. As already described, ICAD is a mouse homolog of human DFF-45. Caspase-3 cleaves DFF-45, and once caspase-activated, deoxyribonuclease (CAD) is released, it can enter the nucleus, where it degrades chromosomal DNA to produce inter-chromosomal DNA fragmentation [30,31]. Figure 4C shows that the exposure of COLO 205 cells to MR-3 causes the degradation of 116 kDa PARP into 85 kDa fragments and induce DFF-45 protein degradation. These protein cleavages were associated with the activation of caspase-3. To further determine if the activation of caspase is necessary for MR-3-induced apoptosis, a pan-caspase inhibitor, z-VAD-FMK, was used to block intracellular protease and MR-3-induced apoptosis was then analyzed by flow cytometry. Results shown in Figure 4D

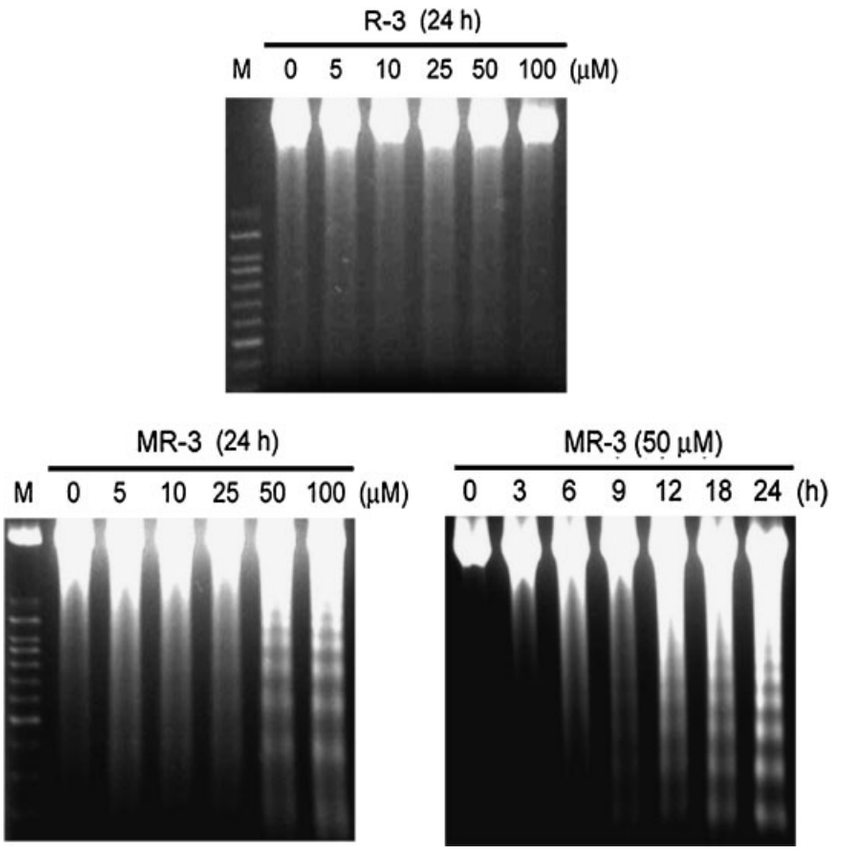

Figure 3. Induction of DNA fragmentation by MR-3 in COLO 205 cells. COLO 205 cells treated with increasing doses of R-3 or MR-3 for 24 h or treated with 50 μM MR-3 for the indicated time, and inter-nucleosomal DNA fragmentation was analyzed by agarose gel electrophoresis. M, 100 base pair DNA ladder size marker. The data presented are representative of three independent experiments.

indicated that the pan-caspase inhibitor (30 μM) significantly inhibited MR-3-induced apoptosis.

Involvement of Mitochondrial Dysfunction, ROS Production, GSH Depression, and Release of Cytochrome-*c* From Mitochondria to Cytosol in MR-3-Induced Apoptosis

It has recently become clear that apoptosis involves a disruption of mitochondrial membrane integrity that is decisive for the cell-death process [16]. We therefore evaluated the effects of MR-3 on the mitochondrial trans-membrane potential ($\Delta\Psi_m$) and the release of mitochondrial cytochrome-*c* into cytosol. We measured $\Delta\Psi_m$ fluorescence using a DiOC6(3) probe monitored via flow cytometry. As shown in Figure 4A, which compares COLO 205 cells exposed to MR-3 and the unexposed control cells, the DiOC6(3) fluorescence intensity shifted to the left from 174.45 to 44.22 and 34.66 in MR-3-induced apoptotic COLO 205 cells at 0.5 h and 1 h, respectively. These results confirmed that MR-3 causes a decrease in mitochondrial trans-membrane potential in COLO 205 cells. ROS have been shown to play an important role in the induction of apoptosis [32]. Results of flow cytometry analysis using DCFH-DA and DHE as fluorescent ROS, H_2O_2, and O_2 indicators show an increase in intracellular peroxide levels in MR-3-treated COLO 205 cells. Increases of intracellular peroxide levels by MR-3 were detected at 0.5 h and markedly increased the mean DCFH-DA fluorescence intensity from 4.71 to 977.94, and DHE fluorescence intensity from 112.79 to 121.89. These data indicate that the increase of ROS species might play a role as an early mediator in MR-3-induced apoptosis. These findings show that MR-3 has an effect on mitochondrial function and the accumulation of ROS. Because the depletion of GSH, a major antioxidant, could trigger apoptosis, it is probably that ROS are involved in DNA damage. As shown in Figure 5A, which compares COLO 205 cells exposed to MR-3 to control cells, a marked reduction of GSH levels was observed using the fluorescent probe, 5-chloromethylfluorescein diacetate (CMFDA). CMFDA fluorescence intensity shifted to the left from 82.28 to 61.17 and 46.32 at 0.5 and 1 h, respectively. The features are indicative of an induction of apoptosis. Caspase-9 binds to Apaf-1 in a cytochrome-*c* and

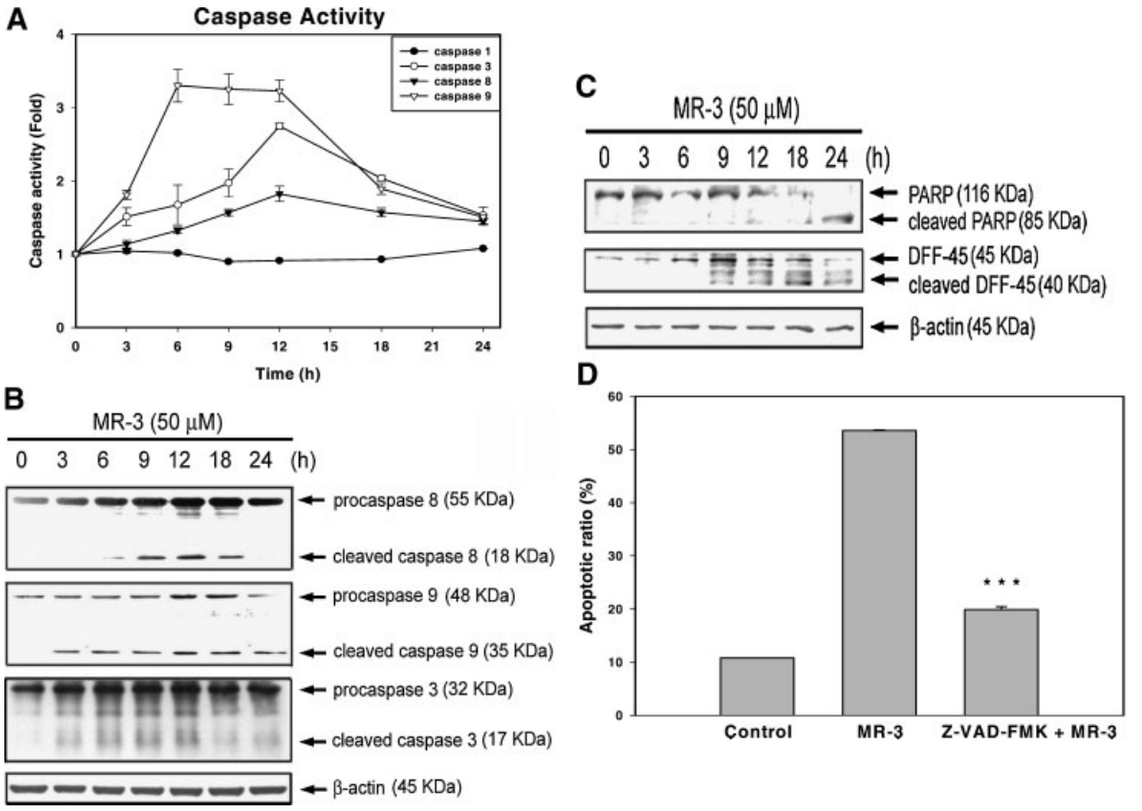

Figure 4. Induction of caspase activities, PARP cleavage, and DFF-45 degradation during MR-3-induced apoptosis in COLO 205 cells. (A) Kinetics of caspase activation in COLO 205 cells. Cells were treated with 50 μM MR-3 for different times. Caspase activities were analyzed as described in the Materials and Methods section. Data represent means ± SD for three determinations. (B) Western blot analyses of pro-caspase-9, -3, and -8 in COLO 205 cells treated with 50 μM MR-3 for different times. Degradation of pro-caspase protein represents its activation. (C) Cleavage of PARP and DFF-45 induced by MR-3 was time dependent. COLO 205 cells were treated as indicated and analyzed by Western blotting as described in the Materials and Methods. (D) COLO 205 cells were pretreated with the caspase inhibitor Z-VAD-FMK for 1 h followed by MR-3 for another 24 h. Apoptosis was examined by flow cytometry. Each value is presented as the mean ± SD.Asterisk denotes a statistically significant decrease compared with values of positive control (***$P < 0.001$).

dATP-dependent fashion to become active and, in turn, cleaves and activates caspase-3 [33]. As shown in Figure 5B, the release of mitochondrial cytochrome-*c* into the cytosol was detected at 1 h in MR-3-treated COLO 205 cells. Therefore, these results suggest that MR-3-induced apoptosis, most probably triggered by production of ROS, which in turn induces dissipation of mitochondrial membrane potential, releases cytochrome-*c* followed by activation of caspase-9.

ROS Production Is Involved in MR-3-Induced Apoptosis

Growing evidence indicates that ROS play an important role in the induction of apoptosis [32]. Therefore, antioxidants such as pyrrolidine dithiocarbamate (PDTC), diphenylene iodonium (DPI), *N*-acetylcysteine (NAC), superoxide dismutase (SOD), allopurinol (ALL), and catalase (CAT) were examined in the current study to determine whether ROS production is an essential event for MR-3-induced apoptosis. As shown in Figure 6A, pretreatment with PDTC (an NFκB inhibitor) and DPI (an NADPH oxidase inhibitor), but not NAC, SOD, and ALL (a xanthine oxidase inhibitor), significantly protects COLO 205 cells from MR-3-induced apoptosis. As shown in Figure 5A, MR-3 induced about a 200-fold increase of intracellular peroxide levels in COLO 205 cells; however, catalase markedly suppressed MR-3-induced apoptosis in a dose-dependent manner (Figure 6B).

Effect of MR-3 on the Expression of Bcl-2 Family, p53, and Fas Protein in COLO 205 Cells

Several gene products are known to be important in controlling the apoptotic process [17]. The imbalance of expression of anti- and pro-apoptotic proteins following stimulation is one of the major mechanisms underlying the ultimate fate of cells in the apoptotic process. We examined the expression of the anti-apoptotic proteins, Bcl-X_L and Bcl-2, and the pro-apoptotic Bad and Bax proteins at different time points in MR-3-treated cells. As shown in Figure 7A, there were marked changes in the expression of Bcl-2 in MR-3-treated cells at 12 h,

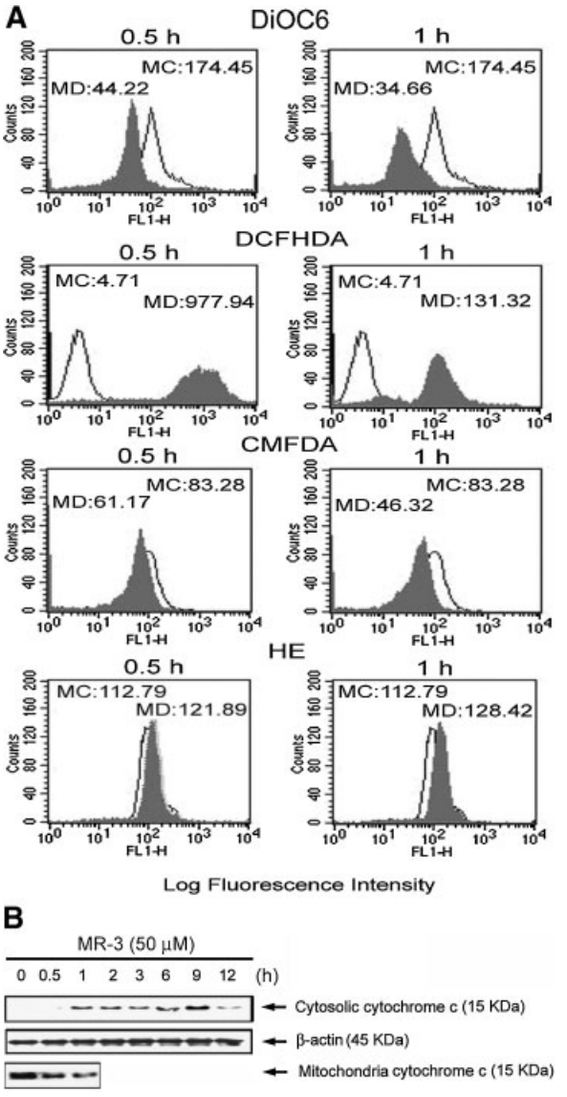

Figure 5. Induction of mitochondrial dysfunction, reactive oxygen species (ROS) generation, cellular content of glutathione (GSH), and cytochrome-*c* release in MR-3-induced apoptosis. (A) COLO 205 cells were treated with 50 μM MR-3 for indicated times and were then incubated with 3,3′-dihexyloxacarbocyanine (40 nM), DCFH-DA (20 μM), CMFDA (20 μM), DHE (20 μM) respectively and analyzed by flow cytometry. Data are presented as log fluorescence intensity. (B) COLO 205 cells were treated with 50 μM MR-3 for different times (0.5, 1, 2, 3, 6, 9, and 12 h). Subcellular fractions were prepared as described in the Materials and Methods section and cytosolic cytochrome-*c* was detected by cytochrome-*c* antibody. This experiment was repeated three times with similar results.

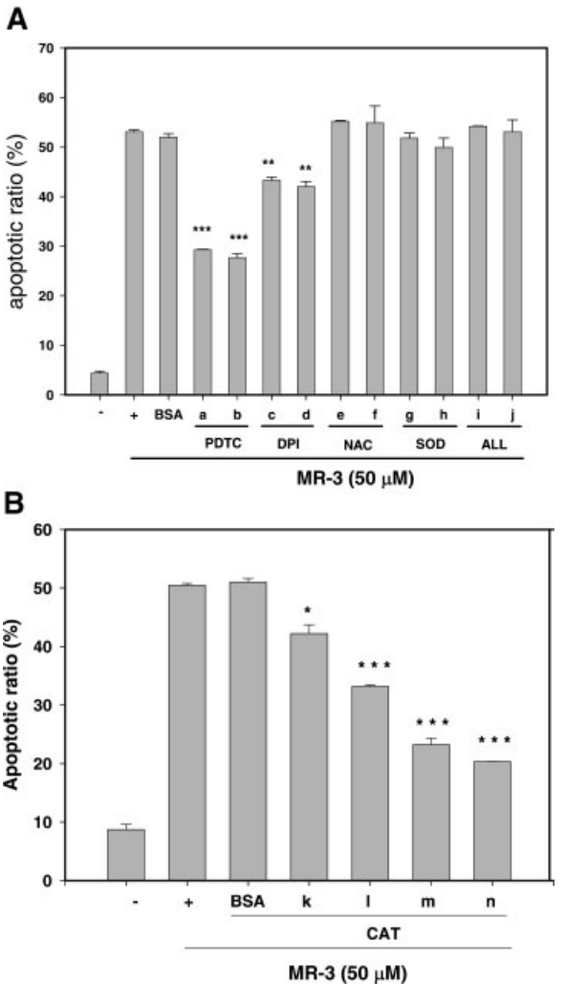

Figure 6. Effects of antioxidants on MR-3-treated COLO 205 cells. (A) COLO 205 cells were treated with different concentrations of PDTC, DPI, NAC, SOD, ALL, and (B) CAT for 1 h followed by MR-3 (50 μM) treatment for another 24 h. The apoptotic ratio was determined by flow cytometry described in the Material and Methods section. Each value is presented as the mean ± SE of three independent experiments. PDTC (a: 20 μM, b: 40 μM), DPI (c: 20 μM, d: 40 μM), NAC (e: 2.5 mM, f: 5 mM), SOD (g: 100 μg/mL, h: 200 μg/mL), ALL (i: 50 μM, j: 100 μM), CAT (k: 50 U/mL, l: 100 U/mL, m: 200 U/mL, n: 400 U/mL). Bovine serum albumin (BSA: 40 μg/mL) used as control. Asterisk denotes a statistically significant decrease compared with values of positive control (*$P < 0.05$, **$P < 0.01$, ***$P < 0.001$).

but no change was observed in the expression of Bcl-X_L. In contrast, there was a marked increase of Bax, expression but no change in the Bad protein level after MR-3 treatment (Figure 7B).

Previous studies demonstrated that the p53 protein is a potent transcription factor, activated and accumulated in response to DNA-damaging agents [34], leading to cell-cycle arrest or apoptosis [35,36]. Figure 7C shows that the p53 protein level was slightly elevated at 1 h following MR-3 treatment of the cells. To assess whether MR-3 promoted apoptosis via a receptor-mediated pathway, the Fas and Fas ligand (FasL) protein levels were determined by Western blotting. The results demonstrated that MR-3 could stimulate the expression of Fas, but not FasL, after treatment with MR-3. Maximum Fas cleavage was detected at 9 h. A marked cleavage of Bid also occurred at this time-point.

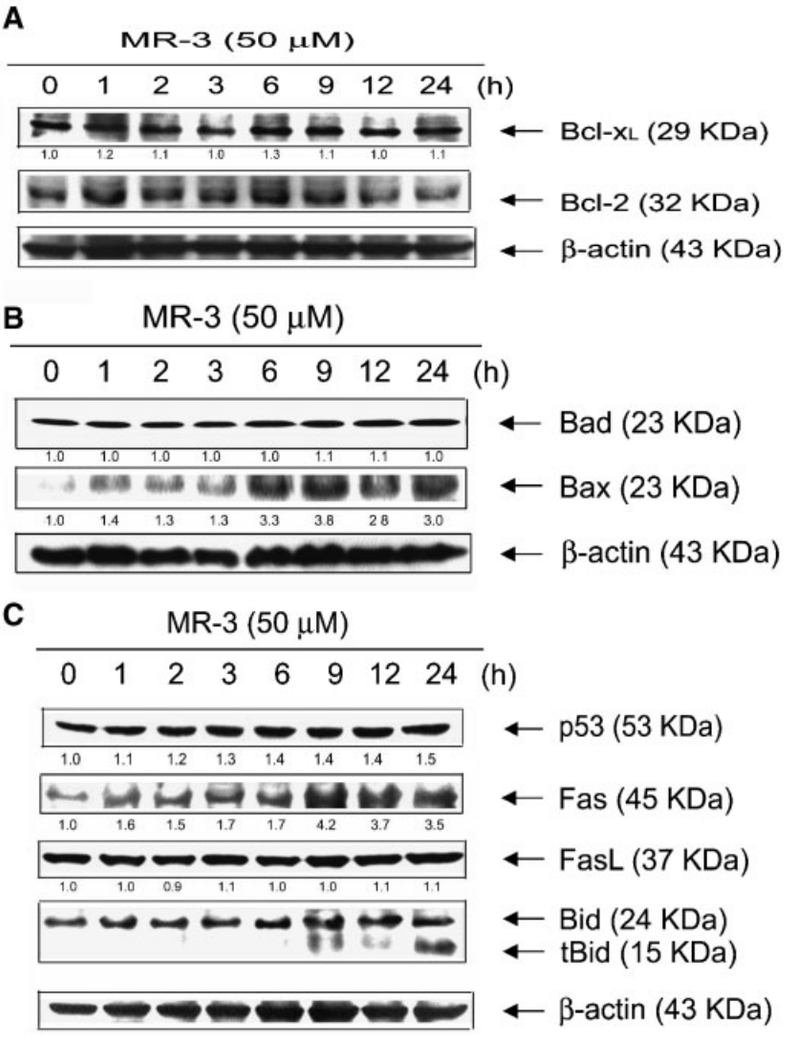

Figure 7. Effect of MR-3 on Bcl-2 protein family, p53, Fas, and FasL expression in MR-3-treated COLO 205 cells. COLO 205 cells were treated with 50 μM MR-3 for indicated times. (A) The expression of Bcl-X_L and Bcl-2, (B) Bad and Bax, (C) p53, Fas, FasL, and Bid was analyzed by Western blotting as described in the Material and Methods section. This experiment was repeated three times with similar results. The values below the figure represent change in protein expression of the bands normalized to β-actin.

MR-3 Inhibits Tumor Growth In Vivo

We further examined the therapeutic efficacy of MR-3 in vivo by treating SCID mice bearing human colorectal carcinoma COLO 205 tumor xenografts, using MR-3 at a concentration of 50 mg/kg. After the establishment of palpable tumors (mean tumor volume, 200 mm^3), animals received intra-peritoneal injections of MR-3 three times per week. Corn oil was used as a negative control. After 23 days, tumor volume in MR-3 was significantly inhibited in comparison with the corn oil-treated controls (Figure 8A). Furthermore, in mice receiving these treatment regimens, no gross signs of toxicity were observed (body weight, visible inspection of general appearance, and microscopic examination of individual organs). The tumor weight and the tumor/body weight ratio were strongly inhibited in the MR-3-treated mice (Figure 8B). Our results provide further evidence that such observations may have significance for cancer chemotherapeutic purposes.

Apoptosis and p53 Plays an Important Role in MR-3-Inhibited Tumor Growth In Vivo

To demonstrate that apoptosis was induced in MR-3-treated tumor tissue, protein was extracted from tumor tissue in the control and MR-3-treated mice. Our results demonstrated that marked increase in the activity of caspase-3 and -9 (but not caspase-1, -2, and -8) occurred in MR-3-treated tumor xenografts (Figure 9A). Furthermore, the morphology of the

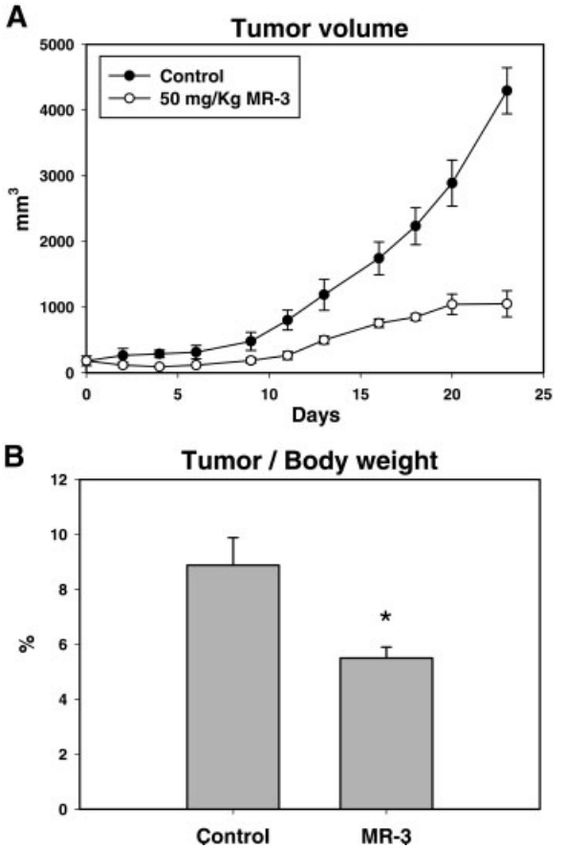

Figure 8. The growth of COLO 205 tumor xenografts in SCID mice was reduced by MR-3 treatment. COLO 205 cells were injected subcutaneously between the scapulas of SCID mice. Once tumor volume reached approximately 200 mm^3, the animal received an injection of 50 mg/kg ip MR-3 or corn oil three times per week for 23 days. (A) Average tumor volume of corn oil-treated ($n = 5$) versus MR-3-treated ($n = 5$) SCID mice, and (B) tumor/body weight ratio were measure at the end of experiment. Five sample were analyzed in each group, and value represent the mean ± SD. Comparisons were subjected to Student's *t*-test. Significantly different at $^*P < 0.05$.

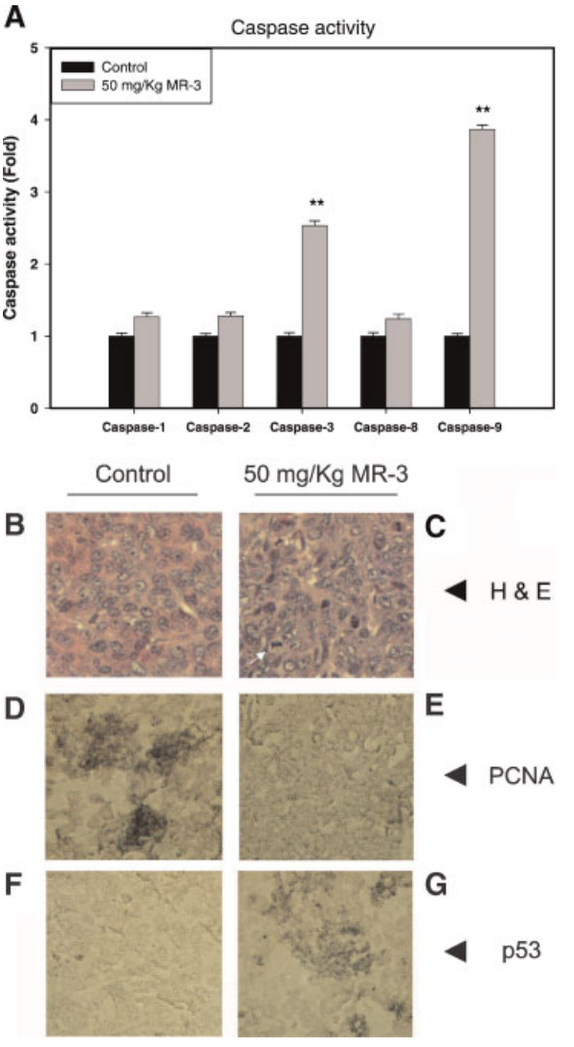

Figure 9. Apoptotic cells were observed in MR-3-treated tumor tissues. (A) The protein extracts were isolated from the frozen tumor tissues and caspase activity was determined. (B) Microscopic view of the paraffin section stained with H & E shown in corn oil (as a control) and (C) MR-3-treated groups. (D) Immuno-histochemical stain analysis of the PCNA protein expression in corn oil (as a control), and (E) MR-3-treated tumor section, and (F) p53 expression in corn oil (as a control), and (G) MR-3-treated tumor section. Magnification 200×. Each value is presented as the mean ± SE of three independent experiments. Significantly different at $^{**}P < 0.01$. The experiments were performed at least three times, and a representative experiment is presented. [Color figure can be viewed in the online issue, which is available at www.interscience.wiley.com.]

apoptotic cells from the tumor tissues was also observed by the H&E staining technique (Figure 9B and C). The apoptotic cells observed in the MR-3-treated group were more significant in tumor tissues compared to the control group (Figure 9D, arrowhead). To further investigate the expression of proliferating cell nuclear antigen (PCNA) and the p53 protein in tumor tissues treated with MR-3, an immuno-histochemical stain technique was performed. As shown in Figure 9, the PCNA protein was significantly inhibited in MR-3-treated tumor tissues (Figure 9D and E). The p53 protein was markedly induced and accumulated in the MR-3-treated group compared with the corn oil-treated tumor tissues (Figure 9F and G). Our results imply that inhibition of tumor cell growth via inhibition of the expression of PCNA and induction of the p53-signaling apoptotic pathway are promoted by treatment with MR-3.

DISCUSSION

In the present study, we have tested the effect of resveratrol and its methoxy derivative (Figure 1) on human cancer cell lines. MR-3 markedly exhibited an inhibitory effect toward COLO 205 cell growth (Figure 2). This study indicates that the difference in

bioactivity of MR-3 is related to the presence and positionality of methoxy groups on the basic resveratrol chemical structure. COLO 205 cells underwent apoptosis following treatment with MR-3, suggesting that apoptosis is the major cause for the growth-inhibitory effect of MR-3. This data should provide synthetic chemists with novel information for the design of anti-tumor agents, and also information to support further biological studies of these modified and unmodified functional groups in the future.

Data generated from this research suggest that MR-3 triggers human colorectal carcinoma COLO 205 cells to undergo apoptosis. As shown in Figure 2, MR-3 is a strong inhibitor of cell viability and causes the potent and rapid induction of apoptosis, concurrent with DNA laddering, chromatin condensation, and apoptotic appearance in COLO 205 cells. This induction of apoptosis occurs within hours, consistent with the view that MR-3 induces apoptosis by activating a pre-existing apoptotic machinery. Indeed, treatment with MR-3 causes an induction of caspase-3 (but not caspase-1), which is associated with the degradation of DFF-45 and PARP, and which preceded the onset of apoptosis. Pretreatment with the caspase-3 inhibitor, Z-VAD-FMK, inhibits MR-3-induced apoptosis, suggesting that apoptosis induced by MR-3 involves a caspase-3-mediated mechanism (Figure 4).

The mitochondrial trans-membrane potential ($\Delta\Psi_m$) is often used as an indicator of cellular viability, and its disruption has been implicated in a variety of apoptotic phenomena [37]. Mitochondria have also been implicated as a source of ROS during apoptosis. Reduced mitochondrial membrane potential has recently been shown to lead to increased generation of ROS and apoptosis [38,39]. This research has demonstrated that MR-3 disrupts the functions of the mitochondria in the early stages of apoptosis, and subsequently coordinates caspase-9 activation (but not caspase-1) through the release of cytochrome-*c*. COLO 205 cells showed increasing ROS production following MR-3 treatment (Figure 5). Therefore, we speculate that intracellular generation of ROS can be an important factor in MR-3-induced apoptosis.

To verify this, we performed experiments confirming the effects of antioxidants on MR-3-mediated apoptosis. Pretreatment with the antioxidants pyrrolidine dithiocarbamate and catalase (used as free-radical scavengers), were found to cause a significant inhibition in MR-3-induced apoptosis; however, the antioxidants NAC, SOD, and ALL did not reverse the apoptotic activity of MR-3 (Figure 6). Catalase has been shown to scavenge ROS through conversion of H_2O_2 to H_2O and O_2. This strongly implies that intracellular peroxide may play a pivotal role in MR-3-elicited apoptotic cell death. However, the exact mechanism by which MR-3 induces intracellular peroxide levels is presently unknown and remains to be investigated.

The Bcl-2 family of proteins, whose members may be anti-apoptotic or pro-apoptotic, regulate cell death by controlling mitochondrial membrane permeability during apoptosis [40,41]. We therefore inferred that the Bcl-2 family of proteins may participate in the seminal event that controls the change in mitochondrial membrane potential, triggering cytochrome-*c* release during apoptosis induced by MR-3. In our study, we found upregulation of Bax expression and the phosphorylation of Bcl-2 during MR-3-induced apoptosis in COLO 205 cells (Figure 7). Consistent with a model in which the ratio of anti-apoptotic to pro-apoptotic proteins determines cellular susceptibility to apoptosis [42], the lower ratio of Bcl-2 to Bax was inversely related to increased incubation times following MR-3 treatment.

The p53 tumor suppressor is predominantly a nuclear transcription factor, activated by various stresses, including chemopreventive agents [43]. Normal p53 function acts as a tumor suppressor, inducing both growth arrest and apoptosis. p53 activates the Fas gene in response to DNA damage by anticancer drugs [44]. Treatment of the COLO 205 cells with MR-3 results in an increase in the level of the p53 protein (Figure 7C). Our findings indicate that MR-3-triggered apoptosis might be caused by increased expression of the Bax and Fas proteins, dependent on the p53 protein, which effects mitochondrial function. These data indicate a possible causal relationship in which the expression of Bax or Fas may be transcriptionally regulated in response to MR-3 treatment. However, this issue requires further elucidation.

Direct evidence to support the in vitro antitumor activity of MR-3 was provided by our *in vivo* study. MR-3 at a dose of 50 mg/kg significantly reduced tumor growth in SCID mice that had been caused by subcutaneous injection of COLO 205 cells. This was accompanied by the appearance of apoptotic cells in tumor tissues, in accordance with the induction of p53 protein expression (Figure 9G). These results suggest that the p53-signaling pathway may be involved in mediating MR-3-induced apoptosis in tumor tissues. No significant cytotoxicity was observed in MR-3-treated SCID mice. Although MR-3 can change the integrity of the mitochondrial membrane by regulating the expression of Bcl-2 family proteins, we do not rule out the possibility that MR-3 can penetrate cells, directly target mitochondria, and thereby increase membrane permeability with an attendant decrease of $\Delta\Psi_m$, accompanied by ROS production. On the basis of this data, we propose an apoptotic mechanism induced by MR-3 (Figure 10). The initial event induced by MR-3 is a likely induction of ROS, based

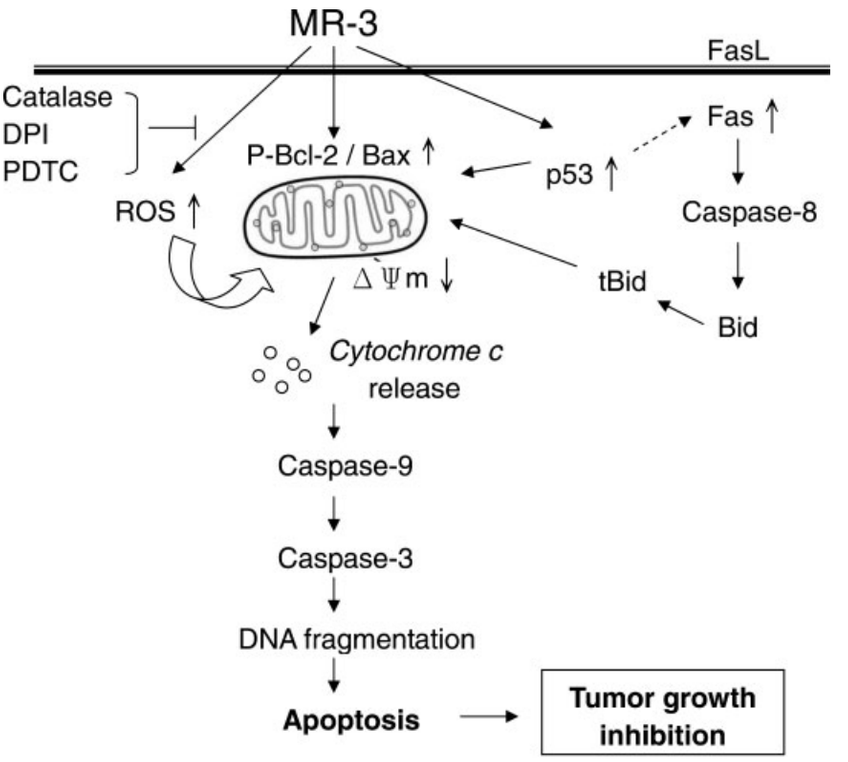

Figure 10. Schematic representation of mechanisms of action by which MR-3-induced apoptosis in COLO 205 cells. The initial event induced by MR-3 may be induction of ROS production and coordinated modulation of Bcl-2 family, followed by reduction in ΔΨm, resulting in cytochrome-c release, and which then leads to the consequent activation of caspase-9, caspase-3, and caspase-8. Alternatively, p53 induced Fas expression drives the activation of caspase-8. Caspase-8 might then indirectly disturb ΔΨm by cleaving Bid and causing the release of cytochrome-c. Activated caspase-3 can further cleave inhibitor of caspase-activated DNase (ICAD), allowing the caspase-activated DNase (CAD) to enter the nucleus and degrade chromosomal DNA. The dashed line indicates this pathway, not investigated in the present study.

on the finding that PDTC, DPI, and CAT prevented apoptosis.

In summary, we have provided the basis for a molecular mechanism of MR-3 in cancer treatment. The potential application of MR-3 to inhibit cancer cell proliferation makes it an attractive agent for colorectal carcinoma research and possibly, treatment.

ACKNOWLEDGMENTS

This study was supported by the National Science Council NSC 95-2321-B-022-001 and NSC 95-2313-B-022-003-MY3

REFERENCES

1. Kelloff GJ, Boone CW, Crowell JA, Steele VE, Lubet R, Sigman CC. Chemopreventive drug development: Perspectives and progress. [Review] [226 refs]. Cancer Epidemiol Biomarkers Prevent 1994;3:85–98.
2. Kang SK, Burnett CA, Freund E, Walker J, Lalich N, Sestito J. Gastrointestinal cancer mortality of workers in occupations with high asbestos exposures. Am J Ind Med 1997;31:713–718.
3. Hirota S. Gastrointestinal stromal tumors: Their origin and cause. Int J Clin Oncol 2001;6:1–5.
4. Strickland L, Letson GD, Muro-Cacho CA. Gastrointestinal stromal tumors. Cancer Control 2001;8:252–261.
5. Jang M, Cai L, Udeani GO, et al. Cancer chemopreventive activity of resveratrol, a natural product derived from grapes. Science 1997;275:218–220.
6. Lu J, Ho CH, Ghai G, Chen KY. Resveratrol analog, 3,4,5,4′-tetrahydroxystilbene, differentially induces pro-apoptotic p53/Bax gene expression and inhibits the growth of transformed cells but not their normal counterparts. Carcinogenesis 2001;22:321–328.
7. Fontecave M, Lepoivre M, Elleingand E, Gerez C, Guittet O. Resveratrol, a remarkable inhibitor of ribonucleotide reductase. FEBS Lett 1998;421:277–279.
8. Joe AK, Liu H, Suzui M, Vural ME, Xiao D, Weinstein IB. Resveratrol induces growth inhibition, S-phase arrest, apoptosis, and changes in biomarker expression in several human cancer cell lines. Clin Cancer Res 2002;8:893–903.
9. Carbo N, Costelli P, Baccino FM, Lopez-Soriano FJ, Argiles JM. Resveratrol, a natural product present in wine, decreases tumour growth in a rat tumour model. Biochem Biophys Res Commun 1999;254:739–743.
10. Folkman J, Watson K, Ingber D, Hanahan D. Induction of angiogenesis during the transition from hyperplasia to neoplasia. Nature 1989;339:58–61.
11. Belleri M, Ribatti D, Nicoli S, et al. Antiangiogenic and vascular-targeting activity of the microtubule-destabilizing trans-resveratrol derivative 3,5,4′-trimethoxystilbene. Mol Pharmacol 2005;67:1451–1459.

12. Kerr JF, Wyllie AH, Currie AR. Apoptosis: A basic biological phenomenon with wide-ranging implications in tissue kinetics. Br J Cancer 1972;26:239–257.
13. Hetts SW. To die or not to die: An overview of apoptosis and its role in disease. JAMA 1998;279:300–307.
14. Jacobson MD, Weil M, Raff MC. Programmed cell death in animal development. Cell 1997;88:347–354.
15. Earnshaw WC, Martins LM, Kaufmann SH. Mammalian caspases: Structure, activation, substrates, and functions during apoptosis. Annu Rev Biochem 1999;68:383–424.
16. Green DR, Reed JC. Mitochondria and apoptosis. Science 1998;281:1309–1312.
17. Merry DE, Korsmeyer SJ. Bcl-2 gene family in the nervous system. Annu Rev Neurosci 1997;20:245–267.
18. Sato T, Hanada M, Bodrug S, et al. Interactions among members of the Bcl-2 protein family analyzed with a yeast two-hybrid system. Proc Natl Acad Sci USA 1994;91:9238–9242.
19. Kluck RM, Bossy-Wetzel E, Green DR, Newmeyer DD. The release of cytochrome c from mitochondria: A primary site for Bcl-2 regulation of apoptosis. Science 1997;275:1132–1136.
20. Bellows DS, Chau BN, Lee P, Lazebnik Y, Burns WH, Hardwick JM. Antiapoptotic herpesvirus Bcl-2 homologs escape caspase-mediated conversion to proapoptotic proteins. J Virol 2000;74:5024–5031.
21. Sathornsumetee S, Rich JN. New treatment strategies for malignant gliomas. Expert Rev Anticancer Therap 2006;6:1087–1104.
22. Kelloff GJ, Lippman SM, Dannenberg AJ, Sigman CC, et al. AACR Task Force on Cancer Prevention. Progress in chemoprevention drug development: The promise of molecular biomarkers for prevention of intraepithelial neoplasia and cancer—A plan to move forward. Clin Cancer Res 2006;12:3661–3697.
23. Semple TU, Quinn LA, Woods LK, Moore GE. Tumor and lymphoid cell lines from a pateint with carcinoma of the colon for a cytotoxicity model. Cancer Res 1978;38:1345–1355.
24. Pan MH, Chen WJ, Lin-Shiau SY, Ho CT, Lin JK. Tangeretin induces cell-cycle G1 arrest through inhibiting cyclin-dependent kinases 2 and 4 activities as well as elevating Cdk inhibitors p21 and p27 in human colorectal carcinoma cells. Carcinogenesis 2002;23:1677–1684.
25. Pan MH, Chang WL, Lin-Shiau SY, Ho CT, Lin JK. Induction of apoptosis by garcinol and curcumin through cytochrome c release and activation of caspases in human leukemia HL-60 cells. J Agric Food Chem 2001;49:1464–1474.
26. Pan MH, Lin JH, Lin-Shiau SY, Lin JK. Induction of apoptosis by penta-O-galloyl-beta-D-glucose through activation of caspase-3 in human leukemia HL-60 cells. Eur J Pharmacol 1999;381:171–183.
27. Ho YS, Duh JS, Jeng JH, et al. Griseofulvin potentiates antitumorigenesis effects of nocodazole through induction of apoptosis and G2/M cell cycle arrest in human colorectal cancer cells. Int J Cancer 2001;91:393–401.
28. Stroh C, Schulze-Osthoff K. Death by a thousand cuts: An ever increasing list of caspase substrates. Cell Death Differ 1998;5:997–1000.
29. Tewari M, Quan LT, O'Rourke K, et al. Yama/CPP32 beta, a mammalian homolog of CED-3, is a CrmA-inhibitable protease that cleaves the death substrate poly(ADP-ribose) polymerase. Cell 1995;81:801–809.
30. Liu X, Zou H, Slaughter C, Wang X. DFF, a heterodimeric protein that functions downstream of caspase-3 to trigger DNA fragmentation during apoptosis. Cell 1997;89:175–184.
31. Sakahira H, Enari M, Nagata S. Cleavage of CAD inhibitor in CAD activation and DNA degradation during apoptosis. Nature 1998;391:96–99.
32. Martindale JL, Holbrook NJ. Cellular response to oxidative stress: Signaling for suicide and survival. J Cell Physiol 2002;192:1–15.
33. Li P, Nijhawan D, Budihardjo I, et al. Cytochrome c and dATP-dependent formation of Apaf-1/caspase-9 complex initiates an apoptotic protease cascade. Cell 1997;91:479–489.
34. Morgan SE, Kastan MB. p53 and ATM: Cell cycle, cell death, and cancer. Adv Cancer Res 1997;71:1–25.
35. Ko LJ, Prives C. p53: Puzzle and paradigm. Genes Dev 1996;10:1054–1072.
36. Levine AJ. p53, the cellular gatekeeper for growth and division. Cell 1997;88:323–331.
37. Marchetti P, Castedo M, Susin SA, et al. Mitochondrial permeability transition is a central coordinating event of apoptosis. J Exp Med 1996;184:1155–1160.
38. Zamzami N, Marchetti P, Castedo M, et al. Sequential reduction of mitochondrial transmembrane potential and generation of reactive oxygen species in early programmed cell death. J Exp Med 1995;182:367–377.
39. Finkel T, Holbrook NJ. Oxidants, oxidative stress and the biology of ageing. Nature 2000;408:239–247.
40. Adams JM, Cory S. The Bcl-2 protein family: Arbiters of cell survival. Science 1998;281:1322–1326.
41. Tsujimoto Y. Role of Bcl-2 family proteins in apoptosis: Apoptosomes or mitochondria? Genes Cells 1998;3:697–707.
42. Oltvai ZN, Milliman CL, Korsmeyer SJ. Bcl-2 heterodimerizes in vivo with a conserved homolog, Bax, that accelerates programmed cell death. Cell 1993;74:609–619.
43. Jimenez GS, Khan SH, Stommel JM, Wahl GM. p53 regulation by post-translational modification and nuclear retention in response to diverse stresses. Oncogene 1999;18:7656–7665.
44. Muller M, Wilder S, Bannasch D, et al. p53 activates the CD95 (APO-1/Fas) gene in response to DNA damage by anticancer drugs. J Exp Med 1998;188:2033–2045.